ESA Climate Change Initiative
River Discharge Precursor
(RD_cci+)

D2. Water Surface Elevation (WSE) Algorithm Theoretical Basis Document (ATBD)

Contract number: 4000139952/22/I-NB

Reference: CCI-Discharge-0005-ATBD-WSE

Issue 2.0 – 12/06/2025

11 rue Hermès, Parc Technologique du Canal — 31520 Ramonville Saint-Agne, France
Tel +33 (0)5 61 39 47 00 Fax +33(0)5 61 75 10 14
www.cls.fr

CHRONOLOGY ISSUES

Issue	Date	Object	Written by
1.0	28/07/23	Initial version	Sylvain Biancamaria et al.
1.1	29/11/23	Data format and architecture sections moved to WSE CRDP release note; added information about differences btw CCI lakes and rivers WSE	Sylvain Biancamaria
1.2	21/02/24	Added in section 4.1 that only one observation per day for merged time series, and in section 3.2 that dates are in UTC time	Sylvain Biancamaria
2.0	30/04/25	The new section 3.3 has been added to described automatic processing chain to compute WSE mono-mission time series. Processing altimeter data for the specific case of Arctic rivers has been added at the end of section 3.2 Section 4 has been reordered to add a section on merging mono-mission WSE time series based on a statistical approach (new section 4.2). A new section (section 5) has been added on WSE uncertainty estimation.	Maxime Vayre, Gabriel Calassou, Elena Zakharova, Sylvain Biancamaria

Checked by	S. Biancamaria - LEGOS	sylvain.biancamaria 22/09/2025
Approved by	Alice Andral - CLS	Pmourot 24/09/2025
Authorized by	Clément Albergel - ESA	clement.albergel 01/10/2025

DISTRIBUTION

Company	Names	Email
ESA	Clément Albergel	clement.albergel@esa.int
~~CLS~~	~~Alice Andral~~	~~aandral@groupcls.com~~
CLS	Philippe Mourot	pmourot@groupcls.com
CLS	Gabriel Calassou	gcalassou@groupcls.com
CLS	Beatriz Calmettes	bcalmettes@groupcls.com
CLS	Daya Ceccone	dceccone@groupcls.com
CLS	Nicolas Taburet	ntaburet@groupcls.com
CLS	Maxime Vayre	mvayre@groupcls.com
CNRM	Kaushlendra Verma	kaushlendra.verma@meteo.fr
CNRM	Simon Munier	simon.munier@meteo.fr
EOLA	Elena Zakharova	zavocado@gmail.com
Hydro Matters	Malik Boussaroque	malik.boussaroque@hydro-matters.fr
Hydro Matters	Laetitia Gal	laetitia.gal@hydro-matters.fr
Hydro Matters	Adrien Paris	adrien.paris@hydro-matters.fr
IRPI	Silvia Barbetta	silvia.barbetta@irpi.cnr.it
IRPI	Christian Massari	christian.massari@cnr.it
IRPI	Paolo Filippucci	paolo.filippucci@irpi.cnr.it
IRPI	Angelica Tarpanelli	angelica.tarpanelli@irpi.cnr.it
LEGOS-CNRS	Sylvain Biancamaria	sylvain.biancamaria@univ-tlse3.fr
LEGOS-CNRS	Fabien Blarel	fabien.blarel@univ-tlse3.fr
LEGOS-IRD	Fernando Niño	fernando.nino@ird.fr
LEGOS-IRD	Fabrice Papa	fabrice.papa@ird.fr
Magellium	Gilles Larnicol	gilles.larnicol@magellium.fr
Magellium	Vanessa Pedinotti	vanessa.pedinotti@magellium.fr
Magellium	Malak Sadki	malak.sadki@magellium.fr
PML	Simis Stefan	stsi@pml.ac.uk
University Exeter - PML	Bachiller Jareno, Nuria	nb748@exeter.ac.uk
University Stuttgart	Omid Elmi	omid.elmi@gis.uni-stuttgart.de
University Stuttgart	Peyman Saemian	peyman.saemian@gis.uni-stuttgart.de
University Stuttgart	Mohammad Tourian	tourian@gis.uni-stuttgart.de

LIST OF CONTENTS

LIST OF TABLES AND FIGURES

REFERENCE DOCUMENTS

[RD1] D.2 Selection of river basins. CCI River Discharge precursor project Document (CCI-Discharge-0004-RP_WP2, Issue 1.1). Available at https://climate.esa.int/documents/2189/D2_CCI-Discharge-0004-RP_WP2_v1-1.pdf

[RD2] D.1 User Requirements Document for CCI River Discharge precursor project (CCI-Discharge-0003-URD, Issue 1.1). Available at https://climate.esa.int/documents/2188/D1_CCI-Discharge-0003-URD.pdf

[RD3] D2.2: Algorithm Theoretical Basis Document (ATBD). CCI Lake project (CCI-LAKES-0024-ATBD, Issue 3.1, 6 July 2022). Available at https://climate.esa.int/media/documents/CCI-LAKES-0024-ATBD_v3.1.pdf

[RD4] D.3 River Discharge (Q) from Altimeters and Ancillary data, multispectral images and data combination - Algorithm Theoretical Basis Document (ATBD). CCI River Discharge precursor project Document (CCI-Discharge-0012-ATBD, Issue 1.2). Available at https://climate.esa.int/documents/2513/CCI-Discharge-0012-ATBD-Discharge.pdf

LIST OF ACRONYMS

ATBD	Algorithm Theoretical Basis Document
CCI	Climate Change Initiative
CNES	Centre National d'Etudes Spatiales
DEM	Digital Elevation Model
ESA	European Space Agency
GDR	Geophysical Data Records
IGDR	Interim Geophysical Data Records
J1	Jason-1
J2	Jason-2
J3	Jason-3
LRM	Low Resolution Mode
OCOG	Offset Centre of Gravity
OLTC	Open-Loop Tracking Command
PISTACH	Prototype Innovant de Système de Traitement pour les Applications Côtières et l'Hydrologie
SAR	Synthetic Aperture Radar
Saral	Satellite with ARgos and ALtika
S3A	Sentinel-3A
S3B	Sentinel-3B
S6	Sentinel-6 Michael Freilich
STC	Short Time Critical
TP	Topex-Poseidon
UTC	Coordinated Universal Time
VS	Virtual Station
WGS84	World Geodetic System 1984
WSE	Water Surface Elevation

1 Introduction

This document describes the theoretical basis for the algorithm used to compute Water Surface Elevation (WSE) from nadir altimeters within the CCI River Discharge precursor project. First, the principles and issue concerning the use of altimeter data over inland waterbodies are presented in section 2. Then, the computation of WSE time series at a single virtual station (VS; i.e., intersection between the satellite ground track and the studied water body/river reach) and from a single altimeter mission is described in section 3. Section 4 presents methods defined to merge time series from different missions and locations.

2 WSE computation from nadir altimeters

2.1 Basic principle of WSE measurements from nadir altimeter

Radar altimeter measurements are used to compute the range (*R* on Figure 1), i.e. the distance between the satellite and the surface of the observed river reach. The altimeter sends a radar pulse at the vertical of the satellite (nadir). Then, it records the radar echo (or waveform) backscattered toward the antenna by the water body below the satellite. This radar waveform is downlinked on the ground and *R* is estimated by post-processing this waveform. If the radar pulse sent by the instrument was a pure Dirac function with a propagation speed equal to the speed of light in vacuum (noted *c* in Eq. 1), then *R* would be easily computed by recording the radar pulse two-way travel time (noted *dt*) and using Eq. 1.

$$R = \frac{1}{2} \cdot c \cdot dt \qquad \text{Eq. 1}$$

Satellite altitude (*H* on Figure 1) is computed thanks to the on-board instruments. *H* is known quite precisely with recent satellite altimeters (below 2 cm; e.g. Couhert et al., 2015). The WSE (*h* on Figure 1) can be computed using Eq. 2.

$$h = H - (R - \Delta R_{propagation} - \Delta R_{geophysical}) \qquad \text{Eq. 2}$$

The term $\Delta R_{\text{propagation}}$ corrects the range *R* from propagation delay occurring when the radar signal propagates through the atmosphere (its speed is smaller than *c* in this environment). $\Delta R_{\text{geophysical}}$ corrects *R* from geophysical signal affecting the measurements (i.e. crustal vertical motions due to the solid Earth and pole tides).

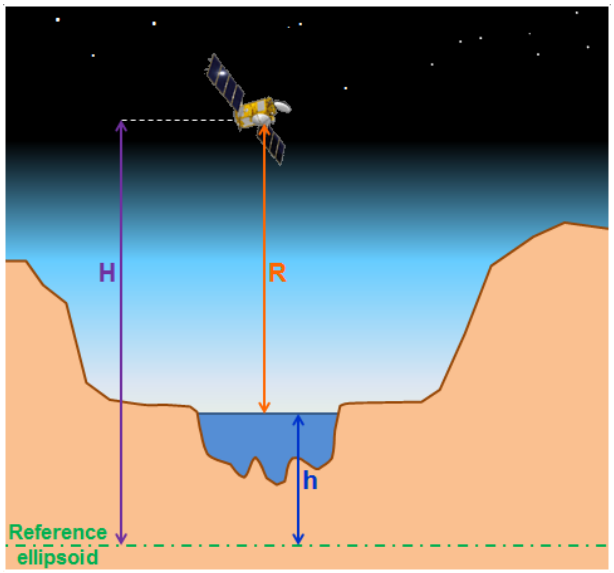

Figure 1. Conceptual view of nadir altimeter and WSE measurements

2.2 Computing the range R from altimeter waveform and its complexity

2.2.1 Tracking window

Due to instrument design, the altimeter can record the backscattered radar signal from only a small portion (labelled "tracking window") of the vertical axis below the satellite. For comparison, the tracking window size of Poseidon-class altimeters (TP, J1 to J3 altimeters) is 60m wide, whereas the satellite orbit altitude is around 1336 km. It is needed to set this vertical tracking window correctly to observe the water body surface. For past missions, the position of this window is computed automatically, based on previously measured waveforms. This tracking method is called "autonomous" or "Closed-Loop" mode. It is conceived to track ocean surface topography, but could fail over continents, which have more important and abrupt topography variations than oceans (e.g. Biancamaria et al., 2018). When the tracking window is not correctly set, then the waveform does contain any backscattered signal from the targeted water body and data over this water body is lost. To overcome this issue, CNES and then ESA conceived another tracking mode, called "Open-Loop" or "Diode/DEM" mode. Rather than updating automatically the tracking window positions, they are set using elevations stored on-board. These elevations come from OLTC tables that are derived from global DEMs and water masks. This mode has been used operationally on J3, S3A/B and S6. For more information on this mode, see for example Desjonquères et al. (2010), Taburet et al. (2020), Le Gac et al. (2021) and the websites: https://sentiwiki.copernicus.eu/web/s3-altimetry-instruments and https://www.altimetry-hydro.eu/.

2.2.2 Retracker

Once the radar waveform backscattered by the continent within the tracking window is recorded by the instrument, it is needed to process it to estimate R for the targeted water body below the satellite nadir. The instrument cannot emit Dirac radar pulses and the instrument "footprint" (defined as the 3-dB antenna beam) is multiple km wide (8km, 18km and 30km diameter for Saral, Envisat and Jason series altimeters, respectively). Therefore, the radar waveform (i.e. the returned power to the instrument as a function of time or, equivalently, of the distance between the satellite and the ground) is not a "simple" pulse but is spread in time (or distance/range). This is due to all the targets on the soil within the instrument footprint, which are located at different distance from the satellite and have different backscatter coefficients. Due to the potentially important heterogeneity of the observed scene below the satellite, contrarily to oceans, retracking the radar waveform to compute accurately R within all the potential targets that backscattered power to the satellite is very difficult over continents. Surface waters

are mainly quasi-specular, they are backscattering much more energy to the satellite than most other soil targets. However, in a few km wide footprint, multiple water bodies might be backscattering energy to the satellite. Besides, some other targets, like wet sand (for example wet riverbanks or ephemeral sand islands that have just been uncovered by water) could also be quite specular. Finally, the recorded waveform is digitalized using a fixed number of bins. These bins cover usually 0.5m distance span (except for Saral/AltiKa for which it is 0.3m and for some mode of Envisat which could then be equal to 0.5m, 2m or 8m).

Radar waveforms over continents are very heterogenous and there is currently no theoretical waveform retracker for continents (which is not the case for open ocean), that can be used to retrack waveforms and retrieve unambiguously the range R for a specific water body overflown by a nadir altimeter. For more information and discussion on this topic, see for example Crétaux et al. (2017). A common empirical retracker algorithm used over continental waters, and available in most nadir altimeters, GDR files is the so-called "Ice-1" or "OCOG" retracker (Wingham et al., 1986; Bamber, 1994). This retracker is not described in this document, nor the reasons why it is commonly used at least over rivers. For more information, the reader is referred to Wingham et al. (1986), Bamber (1994) and, for example, Crétaux et al. (2017).

From this section, it is important to recall that, from a single waveform, there is no certainty that the targeted water body is observed within the tracking window, even if the "Open-Loop" tracking mode helps a lot compared to the former "Closed-Loop" tracking mode, nor that the targeted water body range *R* will be correctly estimated by the retracker algorithm, especially if there are more specular targets nearby. That's why, Biancamaria et al. (2018) highlighted that: 'The ability of an altimeter to observe a river is dependent on river width but is determined to an even greater extent by the "surrounding topography, the observation configuration, previous measurements and the instrument design" (Baup et al., 2014; Biancamaria et al., 2017).' It is therefore very difficult, maybe impossible, to assess beforehand where and when an altimeter provided/will provide usable data on a global scale.

3 Deriving WSE time series from a single mission and virtual station

3.1 Radar nadir Altimeter missions used and concept of virtual stations

The timeline and repeat cycle of all nadir radar altimeter missions used in this study are provided in Figure 2. This figure gathers, through the same color code, missions that were on the same orbit tracks. This means they observe the same locations with the same time repetitiveness. If the TP/J1/J2/J3/S6A observe the same VS every 10 days from 1992 to now, with some time overlaps between consecutive missions, this is not the case for other orbits. The ERS-1/ERS-2/Envisat/Saral 35-days orbit tracks are not sampled since 2016, since Saral satellite is drifting and not maintained on a repeat orbit. Another issue is the absence of time overlap between Envisat on its nominal orbit and Saral launch, leading to a few years' observation gap. S3A and S3B missions are on another orbit, with a better time sampling (27 days), but have been launched quite recently (2016 and 2018, respectively).

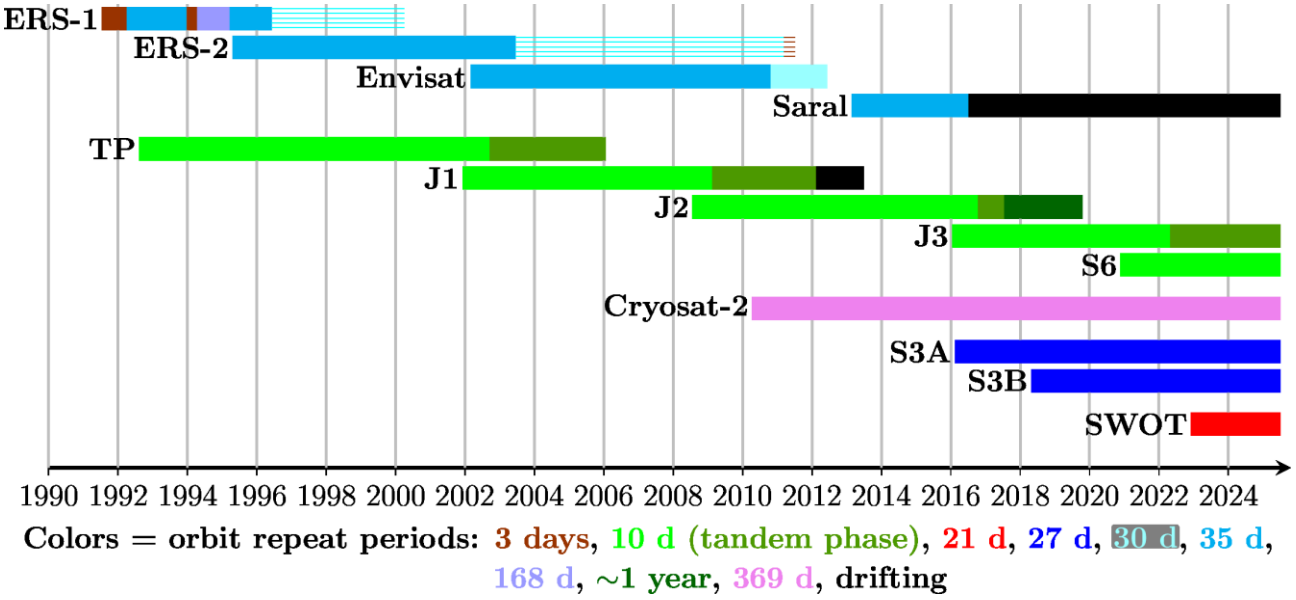

Figure 2. Timeline of the altimetry missions considered in this precursor project. Colors correspond to missions' orbits repeat periods. After June 1996, ERS-1 is in back-up mode and no measurements are recorded and from Mid-2003, altimeter onboard ERS-2 stopped working. That's why the boxplot patterns for these two missions after these dates are changed to show the absence of measurements

The satellite orbit defines both the spatial and temporal sampling of the nadir altimeter mission. They change in opposite directions: the greater the number of tracks in an orbit, the finer its spatial sampling, but the greater its repeat period (i.e. the time taken for the satellite to fly over the same point again), and therefore the coarser its temporal sampling. Therefore, Jason series allows a much better time sampling than other orbits, but the counter part is the scarcity of its spatial sampling (nadir altimeter observing only within the footprint of the instrument at the nadir of the satellite). It means that for some locations chosen [RD1], only observations from altimeters on Envisat orbit could be used, leading to observation gaps (at least between Envisat change of orbit and launch of Saral). Furthermore, due to some technical limitations, satellite ground tracks are controlled to within ± 1 km around their nominal positions for most altimeter missions (for more details, see product handbook for all missions listed on Figure 1).

It should also be noted that the oldest missions are the least accurate. The most important issue arises for J1, which was finer tuned to observe the ocean than TP, resulting in less data acquisition over continental water bodies.

The intersection of the satellite ground track with a targeted water body (e.g. a river reach) is usually referred to as “virtual station” (VS) in scientific literature. Its definition is therefore intrinsically linked with the orbit of the radar nadir altimeter mission considered. The VSs from all available missions tracks near the locations defined in [RD1] have been processed to compute WSE time series.

Dates in the time series are provided at UTC time.

3.2 Algorithm used to compute WSE time series at one virtual station and from one mission with a “manual approach”

WSE is defined as the distance between the surface of water and a reference surface (ellipsoid or geoid). The chosen reference surface is the WGS84 ellipsoid. The geoid is more meaningful from a hydraulic point of view. However, as WSE is not used to compute river slopes in this project and many global to national geoids are available (and multiple versions of a specific geoid might exist), it is better suited to use a mathematically defined reference, i.e. an ellipsoid.

The purpose of this section is to describe the methodology used to compute WSE time series from a single radar nadir altimeter. This precursor project utilised a limited number of WSE time series that had already been computed and made available on the Hydroweb.next database (https://hydroweb.next.theia-land.fr/). This database contains mainly time series from S3A/B, J3 and S6 missions' VSs. It has been needed to extend this database for past missions and VS with current missions not available on Hydroweb.next.

The corrections to be used to compute WSE (see section 2.1 and Eq. 2) are the usual ones considered over continents (Crétaux et al., 2017): ionospheric correction, dry and wet atmospheric corrections, solid Earth correction, and pole tides correction (usual corrections used for inland water bodies) from GDR products provided by space agencies or in the reanalysis products. For TP data available in the PISTACH reanalysis done by CLS, atmospheric corrections are missing at multiple locations. For this mission and at such locations, a climatology produced by LEGOS (from S. Calmant, not published), from the corrections at same locations during the J1 to J3 period, will be used.

To compute time series not available on the Hydroweb.next database, a "manual" approach to select measurements from GDR files will be used. This approach is the same than the one used for "research mode" VS time series on Hydroweb.next (see Hydroweb.next User Manual, https://www.theia-land.fr/wp-content/uploads/2021/06/Handbook_Hydroweb-V2.1-1.pdf, and Santos da Silva et al., 2010). For example, this is done using the AlTiS software, developed at LEGOS/CTOH (https://gitlab.com/ctoh/altis) at LEGOS and Hydro Matters. The main steps of such selection are the followings: 1- define a polygon at the intersection between the satellite ground track and the observed river reach, 2- compute and visualize the WSE (and eventually the backscatter coefficient) for all cycles and measurements within this polygon, 3- remove WSE outliers, 4- for each cycle, compute the median of all selected WSE, and 5- finally export the WSE time series. Concerning step 1, the polygon should cover at least plus or minus 1 km perpendicularly to the ground track (to consider the orbit drift) and few hundreds of meters along track to completely cover the extent of the river reach along the track and contains at least 3 measurement points along the track. Concerning step 3, evident outliers should be removed, for example based on local topography, potential upstream/downstream WSE time series inconsistency, unrealistic WSE amplitude, and presence of other water bodies. However, this "expert judgement" should not be used too frequently and parsimoniously, to avoid removal of extreme events. TP GDR files will come from the PISTACH project. For other missions, GDR files are the ones provided by the space agencies and formatted by the CTOH (http://ctoh.legos.obs-mip.fr).

Differences between the CCI Lake WSE and the precursor CCI River Discharge WSE from the manual approach are the same than differences between "research" Hydroweb.next WSE on lakes and rivers, as described in the Hydroweb.next User Manual and in the CCI lake ATBD [RD3]. The main differences between CCI river WSE and CCI lake WSE are the following: as river WSE are referenced to an ellipsoid and located on a river reach, the geoid slope correction crucial for lake is not applied for rivers WSE; bias between missions (see section 4) is computed differently as there is usually less time series overlaps.

It should be noted that no slope values will be used to correct (the plus or minus 1km) satellite drifts around the theoretical track. There is currently no global river slope product accurate enough to correct this source of errors. When validated SWOT river slope product over at least one year will be available, such type of correction could be considered (i.e., not before August 2024).

In the Arctic, the ice on rivers affects the altimeter waveforms in winter months. The radiometric contrast between snow covered banks and ice (snow-on-ice) covered rivers is usually small. Thus, the backscatter coefficient can be ineffective for the range filtering. The WSE retrievals in winter require an additional step in selection of adequate altimetric measurements. This selection is based on first guess of the seasonal WSE magnitude and on the multi-year statistic of winter measurements at a given VS. In the end of winter, when the ice thermal melting starts (1 to 4 weeks before mechanical breakup), the off-nadir melt ponds and polynyas can result in unrealistically high WSE estimates. To eliminate these

erroneous retrievals, the ice flag, produced from altimetry measurements (Zakharova et al., 2021) and optical images [RD4], is used.

3.3 Algorithm used to compute WSE time series at one virtual station and from one mission with Hysope automatic processing chain

The process used to calculate automatically the mono-mission time series for each station is very similar to the one used with the manual method. The computation is performed from IGDR (or STC) Level-2 data (i.e. Copernicus Data Space Ecosystem | Europe's eyes on Earth for Sentinel-3 data).

Level-2 input altimetry data is first read, selecting high frequency measurements (generally 20 Hz). Ice-1/OCOG retracking algorithm is used.

$$Water\ Surface\ Height = altitude - corrected\ range \quad \text{Eq. 3}$$

With: $corrected\ range = range + wet\ tropospheric\ correction + dry\ tropospheric\ correction + ionospheric\ correction + solid\ earth\ tide\ correction + pole\ tide\ correction$

Water surface height is above the ellipsoid. Ellipsoid reference may differ with respect to the mission. WGS84 for Envisat, Saral and Sentinel-3 and T/P for Topex/Poseidon, Jason-1 and Jason-2. All timeseries are levelled from WGS84, using **Error! Reference source not found.** if needed (correction about 70 cm).

$$\delta = (WSH_{TOPEX} - WSH_{WGS84}) = -((a_2 - a_1)\cos^2(\varphi) + (b_2 - b_1)\sin^2(\varphi)) \quad \text{Eq. 4}$$

The constants of the ellipsoid WGS84 for Envisat and Saral are:

- φ is the latitude coordinate of the Virtual Station,
- a1 = 6 378 137.00 m (WGS84 equatorial radius)
- b1 = 6 356 752.314245 m (WGS84 polar radius)
- a2 = 6 378 136.30 m (T/P equatorial radius)
- b2 = 6 356 751.600563 (T/P polar radius)

Altimetry measurements are selected with respect to VS polygon. Such reference areas are defined from the intersection of the river centerline (i.e. SWOT River Database, SWORD) and theoretical tracks of the mission. High frequency measurements are therefore extracted within these predefined polygons for each VS. The aim of this geographical selection is to use altimetry data located a few kilometers from the VS location.

Altimetry satellites differ from their theoretical position by up to 1km (ground segment constraint). This difference from the theoretical tracks is considered to estimate the water level. For each transect, we estimate the distance from the central position of the SV (provided as metadata). The influence of the local slope is therefore added to the WSH calculation. The local slope is estimated using the IRIS database (IRIS: ICESat-2 River Surface Slope; Scherer et al. 2023) or SWOT profiles from RiverSP Node product. This local slope is also provided as a static value (metadata) for each SV.

$$Water\ Surface\ Height = Water\ Surface\ Height \pm distance * river\ slope \quad \text{Eq. 5}$$

- distance: Curvilinear distance of the current estimate with respect to SV location
- river slope: River local slope estimated from IRIS or RiverSP Node products
- NB: The sign of the correction is defined according to the position of the measurement from the theoretical position (i.e. upstream/downstream with negative/positive slope correction resp.).

The elevation time series is estimated track by track from the WSE estimates. The first editing consists of using sigma0 thresholds. A fixed threshold is defined by VS (mainly depending on the mission). The most echogenic measurements are then selected (corresponding to the highest 50% sigma0). Potential WSE outliers are removed using a 3σ filter on each transect (i.e. selection of measurements from the transect mean +/- 3 times the standard deviation of the WSE distribution on the transect).

A WSE value is computed as the median value of the WSE estimates for the transect. The uncertainty is estimated as the standard deviation of all selected WSE. The measurement is kept if the standard deviation is less than 5 meters. Finally, the measurement (median WSE of the transect) is retained if it respects a constraint of 3σ from the mean and the standard deviation of the whole WSE timeseries (since the start of the time series to the current measurement, particularly useful before the use of OLTC i.e. before the J3 mission).

4 Merged multi-missions altimetry WSE time series

In this precursor project, combined WSEs must be evaluated at least over a few basins with in-situ WSE. Some users indicated in [RD2] that they would be interested in having a combined WSE time series. For river discharge computation from WSE time series and ancillary discharge data, merged WSE at a specific SV is used to compute rating curve. The following sections present different methodologies to compute merged WSE.

4.1 Simple merging methodology

4.1.1 Overall methodology

It is proposed rather to compute a merged WSE at a specific VS, called reference VS. VSs are tied to a mission ground track. So, the reference VS is intrinsically linked to a specific mission orbit. Besides, the intermission bias is dependent, among others, to the considered sensor. That's why it might be better to give priority to the longest mission with valid measurements and with the highest time sampling, but also recent enough to be as accurate as possible. So, **the reference VS should be a J3 VS** (the Jason series is the longest continuous series of altimeter missions, with the highest repeat period, and J3 is the recent enough, as it has been launched in January 2016). However, Jason series ground tracks are sparser than other altimetry missions (the drawback of the higher repeat period). Therefore, **if there is no J3 VS near the location defined in [RD1] to evaluate discharge, then the reference VS should be an Envisat VS** (ERS-2/Envisat and Saral used the same orbit, but as there is no time overlap between Saral and Envisat, which is not the case between Envisat and ERS-2, thus the choice to consider Envisat). **If there is no J3 and Envisat VS available, then a S3A VS should be the reference VS** (however, for this last case, it is doubtful that a 20-year WSE time series could be computed).

It has been decided that the merged time series should have only one measurement per day. If multiple observations are available from single mission time series for a day, the earliest one is kept in the merged time series.

Sections 4.1.2, 4.1.3 and 4.1.4 explain how to merge different time series, depending if they are on the same ground track or not.

4.1.2 Multi-missions on similar orbit and same track (i.e., same VS)

For these cases and if there is a time overlap between consecutive missions, then the mean bias over the common period between the consecutive time series in time is computing and it is removed to get a coherent WSE time series compared to the reference mission. For example, the TP/J1/J2/J3/S6 intermission bias will be computed considering the Jason3 data as the reference. These biases will be

computed considering the mean difference between each mission during the common period. The data in the merged time series during the common period, if the time difference between observation dates is below one hour, will be the WSE from the most recent altimeter. For example, when measurements from J2 and Ja3 are available at the same date, then the J3 data should be provided. Similarly, when both J1 and TP measurements are available at the same date, then the J1 data should be provided. Figures 3 and 4 show some examples of bias corrected time series using this methodology (Figure 4) compared to initially biased time series (Figure 3) for a Jason VS on the Indus River. It should be noted that, for some VS, the first five J3 measurements have important errors. It may be needed to exclude them from the J2/J3 intermission bias computation.

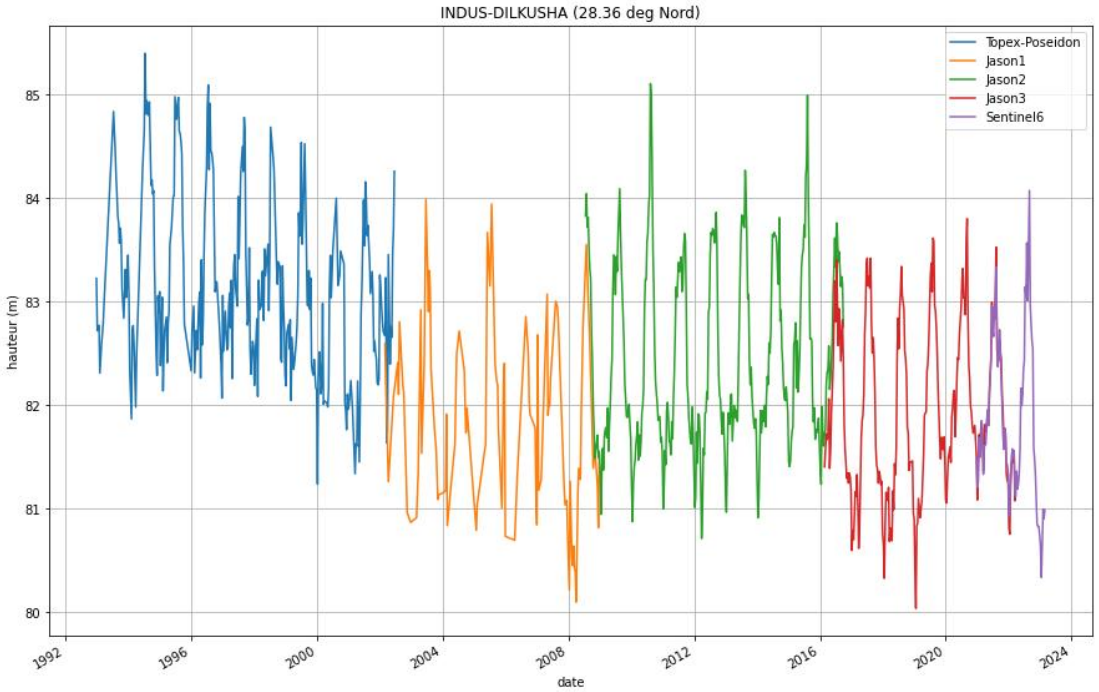

Figure 3. TP/J1/J2/J3/S6 time series without bias correction at VS near Dilkusha on the Indus River

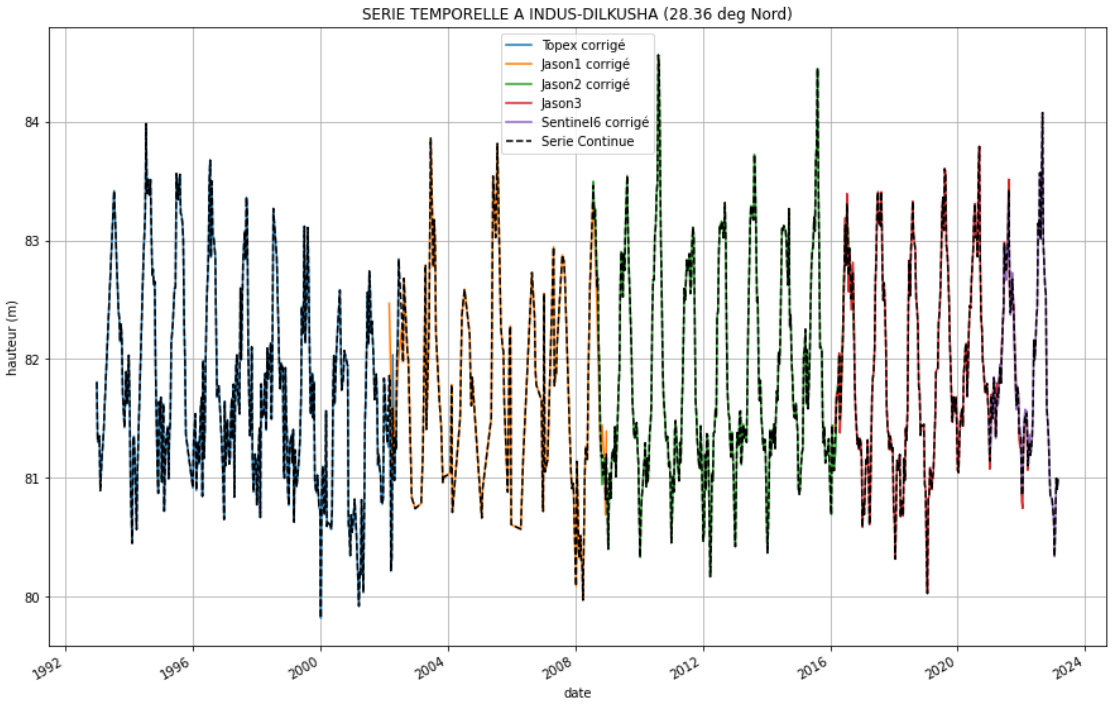

Figure 4. J3 time series and unbiased TP/J1/J2/S6 time series at VS near Dilkusha on the Indus River

4.1.3 Multi-missions not on the same orbit or not on the same track (i.e., on different VS)

Once time series from all missions within the same VS have been merged, then WSE time series from different VSs have to be merged together. A reference VS has to be identified (se section 4.1). In this case, not just a bias correction might be needed. A fit of the relationship between WSE time series at each other VS and the reference VS has to be done. From the scatter plot, over the common period, between the other VS time series and the reference VS time series, will be used to select a linear fit or a Power law fit according to the topology, river characteristics and/or distance between both VSs. These fits have been chosen because, assuming steady and uniform flow, no main tributary between two locations, uniformly varying bathymetry and constant slope of the hydraulic gradient line at these locations, then, due to mass continuity, the relationship between WSE at these two locations is a power-law relationship.

Other VSs should be preferably less than 10km from the reference VS, with no major tributary between the VSs. If for any reason, a VS with a distance much higher than 10km from the reference VS, then using a time lag between the VS and the reference VS should be tested. It will be done using the methodology from Biancamaria et al. (2011): the lag that maximizes the correlation between the reference VS time series and the lagged VS time series.

To concatenate different time series, first data over common overlapping time period(s) between different time series should be considered. These data might not be acquired at the same dates between these different time series. It will be needed to interpolate observations at the same dates to compute the fit (or at least the bias). It will be done by interpolating time series with the highest time sampling to the dates from the time series with the coarsest time sampling, over the common time span. If the time series have the same time sampling, then time series from the other VS will be interpolated to the dates of the reference VS.

4.1.4 Merging time series without time overlap

In order to avoid this case, as much time series as possible should be gathered, rather from the same VSs or from different VS(s) from all altimetry missions considered in this project. Methodology from sections 3.1 to 3.3 should be applied, over consecutive and overlapping in time series starting from the reference VS with the reference satellite mission.

However, the case of consecutive time series with no time overlap might occur (for example, this is the case between Envisat and Saral or TP and J2, if no J1 data could be used). In this case, two methods to correct the bias between non-overlapping missions have been tested. The first is the "average long-term method" that consists of computing the average over the entire time series of the two consecutive missions. The difference between the two averages is used to compute the bias enables to get coherent WSE over the reference VS. The second approach is the "climatology method". A monthly climatology (i.e., all data acquired in January over the whole time series should be average and provided for the month of January in the climatology, similar for the other months) is computed for both consecutive time series. The mean difference (i.e., the average over twelve months of the two monthly climatology's subtractions) between these two climatologies is used to compute the bias and get coherent WSE over the reference VS. The comparison of both methods near Kinshasa station (Congo basin) revealed that they provide similar results (e.g., 0.158 m and 0.156 m from the average long-term and climatology methods respectively between Envisat and Saral missions). Therefore, the monthly climatology method has been chosen to compute bias in this case. For cases with important extreme events or short high flow period (< 1 or 2 months), then 10% of the highest data in the time series will be removed, before computing the monthly climatology or remove the month with the highest value in the climatology.

Computing monthly discharge time series is a goal in [RD2], but there is no similar requirement on WSE product. Therefore, no monthly WSE time series will be computed.

4.2 Stochastic method to merge WSE time series

Before starting the data merging calculation, water level estimates are first referenced to the geoid, as river slope is used. Water surface elevation refers to the level above the geoid:

$$Water\ Surface\ Elevation = Water\ Surface\ Height - geoid \quad \text{Eq. 6}$$

EGM08 is used as ancillary data to calculate the geoid value for a given location. The grid resolution is 1x1 (minute)^2 and downloaded from http://earth-info.nga.mil/GandG/wgs84/gravitymod/egm2008/egm08_wgs84.html.

4.2.1 Overall methodology

As performed in section 4.1, we want to merge WSEs at virtual stations location, but using a stochastic approach inspired by the work of Nielsen et *al*. (2022). The virtual stations are located at the same locations as those defined for the simple merging method (see section 4.1). However, it is important to note that WSEs can be estimated at any point on the section of river studied.

The merged series includes a measurement every five days, and the altimeter observations used can be more than a hundred kilometres from the station.

The following sections explain how altimetry data are merged.

4.2.2 Merging process

The merging process is based on a space-time model that simulates water level variations at a given point in relation to observations made in its vicinity. The estimation of these variations depends on the

statistical formalism of Maximum Likelihood. The space-time model is defined by several conditions. Firstly, it is assumed that the reconstructed time series follow an auto-regressive process of order 1 (AR1). This a stationary process allows first-order simulation of seasonal behaviour of water level variations, η, such that:

$$\eta_{t_i} = \rho\eta_{t_{i-1}} + \xi_i, \quad i = 1, \dots, N \qquad \text{Eq. 7}$$

Where ρ is a constant defined between -1 and 1, N is the number of time steps and ξ_i is an error term following a normal distribution $\mathcal{N}(0, \sigma_\varepsilon^2)$. The time steps of the AR process are equidistant.

Then, each water level is defined by the following direct model:

$$h_i = \eta_{t_i}\alpha_{\theta_\alpha}(x_i) + \tau_{\theta_\tau}(x_i) + \beta(sat_i) + \varepsilon_i \qquad \text{Eq. 8}$$

Where α is a scaling factor to weight variations in water levels according to river bathymetry, τ represents the mean elevation at a position x_i, β represents the inter-mission bias and ε_i is the error term following a normal distribution $\mathcal{N}(0, \sigma_{obs}(sat_i)^2)$. The terms τ and α are interpolated in the state vector θ as a function of the position of the measurement along the curvilinear abscissa of the river.

The parameters of equations 3 and 4 are estimated using Maximum Likelihood to minimize the error terms ξ and ε by maximizing their negative log l:

$$l = l_\eta + l_{obs} = -lnP(\hat{\xi}) - lnP(\hat{\varepsilon}) \rightarrow min. \qquad \text{Eq. 9}$$

Where:

$$\mathrm{l}_\eta = \frac{1}{1-\rho^2} \times \left\| \{\eta_{t_i}\}_{i=2,\dots,N} - \{\rho\eta_{t_j}\}_{j=1,\dots,N-1} \right\|^2, \qquad \text{Eq. 10}$$

$$l_{obs} = \left(H - \widehat{H}\right)^T C_{sat}^{-1} \left(H - \widehat{H}\right). \qquad \text{Eq. 11}$$

P is a normal probability density function (PDF), H is a vector of size N containing the elevations measured by altimetry, $\widehat{H}$ contains the modelled water heights h. C_{sat} is a variance-covariance matrix of uncertainties in altimetry measurements σ_{obs}^2.

4.2.3 Problem initialization

Water level variations (η) are randomly initialized using the R package (TMB) (Kristensen et *al.* 2016). This package applies a Laplace approximation to generate these random effects over the different epochs to make the model robust.

The height variation $\eta_{t=0}$ takes a value of 1e-5 (see Nielsen et *al.,* 2022).

The constant ρ is initialized as equal to 1. α is initialized as a vector composed of 1, and the inter-mission bias β is initialized as zero. Unlike the model developed by Nielsen et al 2022, the mean river profile is not estimated during inversion. This is defined from SWOT RiverSP Nodes data (SWOT, 2024) based on SWORD (Altenau et *al.* 2021). The resolution of the profile along the curvilinear abscissa is 200 meters. To reduce the signal-noise ratio, WSH are re-computed using a sliding median at one kilometre resolution along of the curvilinear abscissa. This treatment only concerns SWOT RiverSP data used to constraint the problem in space. RiverSP Nodes data used as observations are those present at native resolution (200 m). However, SWOT data have only been available since the end of 2023 and so do not capture the full range of hydraulic variations in the river, so the median profiles generated are likely to be biased. This bias is therefore incorporated into θ, the state vector, such as.

$$h_i = \eta_{t_i}\alpha_{\theta_\alpha}(x_i) + [\tau_{\theta_\tau}(x_i) + \beta_{\theta_{\beta_\tau}}(x_i)] + \beta(sat_i) + \varepsilon_i \qquad \text{Eq. 12}$$

4.2.4 Outlier identification

Altimeter measurements can include several outliers that will degrade the model performances. The same procedure as that used in Nielsen et *al.*, 2022 was used to make the model more robust. We apply a weight to each observation to minimize the influence of erroneous observations. The weight associated with each observation is calculated using the following expression:

$$w_i = \begin{cases} \frac{1-\Phi_{\sigma=\sigma_{sat_i}}(|H_i-\widehat{H_i}|)}{p}, & si\ \left(1-\Phi\left(|H_i-\widehat{H_i}|\right)\right) < p, \\ 1 & otherwise \end{cases} \quad \text{Eq. 13}$$

Where Φ represents a cumulative normal distribution. The weights w are initialized to 1 and then be recalculated at each iteration.

5 Uncertainty on WSE time series

5.1 Single mission time series

Uncertainty is not provided in the time series. However, the standard deviation of all WSE selected as valid (see sections 3.2 and 3.3) in the SV polygon is provided for each observation date.

5.2 Merged time series

The WSEs estimated by the stochastic merge method can be characterized as PDFs at each time step, i.e. defined by a mean and a standard deviation representing the probabilistic dispersion of the estimated parameters, also known as the standard error, with respect to the various uncertainties present in the problem.

These uncertainties are calculated by maximizing the log likelihood l such that:

$$Var(\hat{\theta}) \approx \left[-\nabla^2\, l(\hat{\theta})\right]^{-1} \quad \text{Eq. 14}$$

6 References

Altenau, E.H., Pavelsky, T.M., Durand, M.T., Yang, X., Frasson, R.P. de M., Bendezu, L., 2021. The Surface Water and Ocean Topography (SWOT) Mission River Database (SWORD): A Global River Network for Satellite Data Products. Water Resources Research 57, e2021WR030054. https://doi.org/10.1029/2021WR030054

Bamber J. (1994). Ice sheet altimeter processing scheme. International Journal of Remote Sensing, 15, 925-938.

Baup F., F. Frappart, and J. Maubant (2014). Combining high-resolution satellite images and altimetry to estimate the volume of small lakes. Hydrology and Earth System Sciences, 18, 2007–2020, http://dx.doi.org/10.5194/hess-18-2007-2014

Biancamaria S., F. Hossain, and D. P. Lettenmaier (2011). Forecasting transboundary flood with satellites. Geophysical Research Letters, 38, L11401, doi:10.1029/2011GL047290

Biancamaria S., F. Frappart, A.-S. Leleu, V. Marieu, D. Blumstein, J.-D. Desjonquères, F. Boy, A. Sottolichio, and A. Valle-Levinson (2017). Satellite radar altimetry water elevations performance over a 200 m wide river: evaluation over the Garonne River. Advances in Space Research, 59(1), 128-146, http://dx.doi.org/10.1016/j.asr.2016.10.008

Biancamaria S., T. Schaedele, D. Blumstein, F. Frappart, F. Boy, J.-D. Desjonquères, C. Pottier, F. Blarel and F. Niño (2018). Validation of Jason-3 tracking modes over French rivers. Remote Sensing of Environment, 209, 77-89, doi :10.1016/j.rse.2018.02.037

Couhert A., L. Cerri, J.-F. Legeais, M. Ablain, N.P. Zelensky, B.J. Haines, F.G. Lemoine, W.I. Bertiger, S.D. Desai, M. Otten (2015). Towards the 1 mm/y stability of the radial orbit error at regional scales. Advances in Space Research, 55 (1), 2-23, http://dx.doi.org/10.1016/j.asr.2014.06.041

Crétaux J.-F., K. Nielsen, F. Frappart, F. Papa, S. Calmant & J. Benveniste (2017). Hydrological applications of satellite altimetry: rivers, lakes, man-made reservoirs, inundated areas in Satellite Altimetry Over Oceans and Land Surfaces, Earth Observation of Global Changes (éd. Stammer, D. & A. Cazenave) 459-504 (CRC Press, Boca Raton, USA). isbn: 978-1-4987-4345-7.

Desjonquères J.D., G. Carayon, N. Steunou, J. Lambin (2010). Poseidon-3 radar altimeter: new modes and in-flight performances. Marine Geodesy, 33(S1), 53-79, https://doi.org/10.1080/01490419.2010.488970

Kristensen, K., Nielsen, A., Berg, C.W., Skaug, H., Bell, B.M., (2016). TMB: Automatic Differentiation and Laplace Approximation. Journal of Statistical Software, 70, 1–21. https://doi.org/10.18637/jss.v070.i05

Le Gac S., F. Boy, D. Blumstein, L. Lasson and N. Picot (2021). Benefits of the Open-Loop Tracking Command (OLTC): Extending conventional nadir altimetry to inland waters monitoring. Advances in Space Research, 68:2, 843-852, https://doi.org/10.1016/j.asr.2019.10.031

Nielsen, K., Zakharova, E., Tarpanelli, A., Andersen, O.B., Benveniste, J., 2022. River levels from multi mission altimetry, a statistical approach. Remote Sensing of Environment 270, 112876. https://doi.org/10.1016/j.rse.2021.112876

Santos da Silva J., S. Calmant, O. Rotuono Filho, F. Seyler, G. Cochonneau, E. Roux and J. W. Mansour (2010). Water Levels in the Amazon basin derived from the ERS-2 and ENVISAT Radar Altimetry Missions. Remote Sensing of the Environment, 114, 2160-2181, doi:10.1016/j.rse.2010.04.020

Scherer D., C. Schwatke, D. Dettmering and F. Seitz (2023). ICESat-2 river surface slope (IRIS): A global reach-scale water surface slope dataset. Scientific Data, 10, 359. https://doi.org/10.1038/s41597-023-02215-x

Surface Water Ocean Topography (SWOT). 2024. SWOT Level 2 River Single-Pass Vector Data Product, Version C. Ver. C. PO.DAAC, CA, USA. Dataset accessed [2025-04-28] at https://doi.org/10.5067/SWOT-RIVERSP-2.0

Taburet N., L. Zawadzki, M. Vayre, D. Blumstein, S. Le Gac, F. Boy, M. Raynal, S. Labroue, J.-F. Crétaux and P. Femenias (2020). S3MPC: Improvement on Inland Water Tracking and Water Level Monitoring from the OLTC Onboard Sentinel-3 Altimeters. Remote Sensing, 12(18), 3055, https://doi.org/10.3390/rs12183055

Wingham, D.J., Rapley, C.G., Griffiths, H., 1986. New techniques in satellite altimeter tracking systems. In: ESA (Ed.), Proceedings of IGARSS'86 Symposium, Zürich, 8–11 September 1986, SP-254, pp. 1339-1344

Zakharova E., S. Agafonova, C. Duguay, N. Frolova, A. Kouraev (2021). River ice phenology and thickness from satellite altimetry: potential for ice bridge road operation and climate studies. The Cryosphere, 15(12), 5387-5407, https://doi.org/10.5194/tc-15-5387-2021